An Acad Bras Cienc (2025) 97(2): e20241069 DOI 10.1590/0001-3765202520241069
Anais da Academia Brasileira de Ciências | *Annals of the Brazilian Academy of Sciences*
Printed ISSN 0001-3765 I Online ISSN 1678-2690
www.scielo.br/aabc | www.fb.com/aabcjournal

BIOMEDICAL SCIENCES

Encapsulation of *Eucalyptus tereticornis* extract in polylactic-co-glycolic acid nanoparticles: standardization, optimization and cell viability

MARIA C. CELY-GARCIA, DIANA Y. ESPINEL-PABÓN, NANCY JAIMES-MENDEZ, NORMAN BALCAZAR-MORALES & EDWIN A. MURILLO-RUIZ

Abstract: *Eucalyptus tereticornis* extract is a promising drug for the treatment of type 2 diabetes mellitus and obesity, showing *in vitro* effects, such as increased glucose uptake and reduced lipid storage. However, its *in vivo* efficacy has been demonstrated only when administered intraperitoneally. Thus, this study focused on standardisation and optimisation of the preparation of polylactic-co-glycolic acid 50:50 nanoparticles (NPs). The size distribution of the NPs, polydispersity index, and zeta potential were evaluated to identify the NPs with the best encapsulation efficiency and loading capacity based on a first-order design using the response surface methodology. To evaluate cell viability of the NPs, *in vitro* viability assessments were performed using C2C12, 3T3-L1, HepG2, and J774A.1 cell lines and the 3-(4,5-dimethylthiazol-2-yl)-2,5-diphenyltetrazolium bromide assay. The highest encapsulation efficiency and load capacity were 81.569 ± 1.798% and 1.885 ± 0.042%, respectively. These results confirmed the effective encapsulation of *Eucalyptus tereticornis* extract and the interactions between the components of the system. Finally, none of the evaluated concentrations negatively affected the cell line viability, confirming the reproducibility of the method with great pharmacological potential. In addition, this model can be used to develop nanoformulations that efficiently improve response.

Key words: *Eucalyptus tereticornis*, nanoencapsulation, optimization, PLGA, standardization.

INTRODUCTION

Type 2 diabetes mellitus (T2DM) and obesity are public health problems that affect many people worldwide (Alegría et al. 2008, Heredia & Cabriales 2022). The incidence of these diseases has been increasing at an alarming rate. In 2016, it was estimated that over 650 million people were obese and 540 million people worldwide had diabetes, with more than 90% having T2DM (IDF 2021, WHO 2021).

Despite advances in conventional treatments, including changes in diet, increased physical activity, and medication, there is still a need to identify more effective and accessible therapeutic alternatives, particularly in countries with limited resources. Phytotherapy has emerged as an excellent alternative owing to the biodiversity of plants with therapeutic properties (Maldonado et al. 2020).

Recent studies have shown that *Eucalyptus tereticornis* leaves contain a triterpene-rich extract composed of ursolic acid lactone (UAL), oleanolic acid (OA), and ursolic acid (UA), named OBE100. This extract reduces fasting glycemia, insulin resistance, and adipose tissue inflammation in murine model of diet-induced obesity. However, oral administration has limitations, probably owing to the low solubility

and bioavailability of natural pentacyclic triterpenes (Acín et al. 2021).

Synthetic polymers that produce NPs for drug delivery are an efficient alternative for increasing the bioavailability of pharmaceutically active ingredients. An example of such polymers belong to the polyester family, such as poly (lactic acid) (PLA), poly(e-caprolactone), and poly (glycolic acid) (PGA). These are particularly interesting in the biomedical field because of their biocompatibility and biodegradability. Specifically, poly (D, L-lactic-co-glycolic acid) (PLGA) has been approved by the Food and Drug Administration (FDA) for use in human pharmaceuticals (Surya & Bhattacharyya 2021, Wan et al. 2023). PLGA is widely used in drug delivery systems because it is biodegradable, decomposes quickly, lacks intrinsic immunogenicity, and is easy, stable, and safe to produce. The decomposition rate of PLGA depends on the ratio of PLA (hydrophobic) to PGA (hydrophilic) in the copolymer (Gaspar et al. 2018). Currently, pharmaceutical products based on this polymer are commercially available (Sánchez et al. 2020). One of the most commonly used methods for NP fabrication is the emulsion-evaporation method (EEM). EEM allows the encapsulation of water-soluble and fat-soluble substances with a high encapsulation efficiency (EE), good physical and chemical stability (Surya et al. 2021). This is a simple and effective methodology for obtaining NPs of small and uniform sizes, which is crucial for determining drug release and bioavailability (Sánchez et al. 2020). Scaling up for large-scale production is relatively easy, making it attractive for research and industrial applications (Gaspar et al. 2018).

Properties such as composition, size (molecular weight), glass transition temperature, and degree of crystallinity affect the mechanical strength of the polymers. This defines their stability and biodegradation profile (Kamaly et al. 2016, Samani & Taghipour 2015) and determines the characteristics of the nanosystems. For example, the composition of co-glycolic acid (PGA) in co-glycolic lactic acid (PLGA) affects its hydrophilicity, degradation rate, crystallinity, encapsulation efficiency, and release profile (Sanchez et al. 2020). The molecular weight has a direct effect on the particle size and degradation rate. The molecular weight of the polymer is inversely proportional to the particle size and directly proportional to the degradation rate.

In this context, OBE100 nanoformulation was optimized using 50:50 PLA-PGA of 24 and 38 KDa, respectively, and prepared by solvent emulsion-evaporation. It resulted in the formation of hydrophobic core-shell polymeric NPs, where OBE100 extract molecules of this nature were encapsulated. Ursolic acid and oleanolic acid, which are more hydrophobic and account for 58% of the OBE100 extract, interacted with the lactic acid (PLA) moiety of PLGA, directing them toward the interior of the particle. Ursolic acid lactone, which is less hydrophobic and represents 16% of the extract, interacted with the PGA moiety of the polymer and was located in the outermost part of the NPs. This formulation released up to 80% of ursolic acid lactone, but only 35% of oleanolic and ursolic acid in simulated media in the first 6 h (Escobar et al. 2023).

Recent studies indicate that *Eucalyptus tereticornis* extract exhibits high encapsulation efficiency and loading capacity when formulated with PLGA NPs. Based on these findings, our research aims to enhance these nanoformulations by exploring new experimental conditions to standardize and optimize the encapsulation process of the OBE 100 extract in 50:50 PLGA NPs, using 2.0-2.5 KDa polymers. This optimization focuses on improving the stability and bioavailability of the extract by fine-tuning parameters, such as particle size, polydispersity index, and zeta potential, using a response

surface methodology approach. Additionally, we evaluated the effect of the encapsulated NPs on the viability of C2C12, 3T3-L1, HepG2, and J774A.1 cell lines.

Our ultimate goal was to achieve release profiles of the compounds in the OBE100 extract that closely matched those of the pure, unencapsulated extract. In doing so, we aimed to address metabolic abnormalities associated with obesity and enhance the antihyperglycemic and antidiabetic effects of the extract, potentially by regulating the amount of active principle delivered.

ABBREVIATIONS

A_C: PLGA NPs Without OBE100
A_E: PLGA NPS Encapsulated with OBE100
ANOVA: Analysis of variance
DF: Degrees of freedom
DLS: Dynamic light scattering
DMEM: Dulbecco's modified Eagle medium
DMSO: Dimethyl sulfoxide
EE: Encapsulation efficiency
EEM: Emulsion-evaporation method
FA: Ferulic acid
FBS: Fetal bovine serum
FDA: Food and Drug Administration
GENMOL: Molecular Genetics Research Group
HPLC: High-performance liquid chromatography
IBMX: 3-Isobutyl-1-methylxanthine
LbL: Layer-by-layer assembly
LC: Loading capacity
LSD: Minimum significant differences
MS: Mean squares
MSR: Method of surface response
MTT: 3-(4,5-dimethylthiazol-2-yl)-2,5-diphenyltetrazolium bromide assay
Mw: Molecular weight
NPs: Nanoparticles
OA: Oleanolic acid
OBE100: Fraction composed of UAL, OA, UA
PDI: Polydispersity index
PEG: Polyethylene glycol
PGA: Glycolic acid
PLA: Lactic acid
PLGA: Poly(D,L-lactic-co-glycolic acid)
PZ: Z potential
R^2: Multiple correlation coefficients
ROS: Reactive oxygen species
SD: Standard deviation
SS: Sum of squares
T2DM: Type 2 diabetes mellitus
UA: Ursolic acid
UAL: Ursolic acid lactone

MATERIALS AND METHODS

Materials

Previously characterized OBE100, which is composed of a triterpene-rich fraction of UA, OA, and UAL, was supplied by the GENMOL laboratory of the Universidad de Antioquia. PLGA Resomer® RG (50:50 M_w: 2.0-2.5 kDa), hereafter referred to as polymer A, was purchased from Evonik-Alemania. Ethyl acetate, ethanol, kolliphor® P188, dimethyl sulfoxide (DMSO) and (+)-α-tocopherol were supplied by Merck. Spectra/Por (Repligen, USA) supplied the 12-14 kDa dialysis membranes. The mouse muscle cell line C2C12 CRL-1772™, mouse embryonic fibroblasts 3T3-L1 CL-173™, human hepatocellular epithelial tissue HepG2 HB-8065™, and mouse macrophages J774A.1 HB-TIB-67™ were supplied by the American Type Culture Collection. Cell viability was assessed using the 3-(4,5-dimethylthiazol-2-yl)-2,5-diphenyltetrazolium bromide (MTT) (Sigma-Aldrich, St. Louis, Mo, USA), and the absorbance was measured using a Varioskan LUX microplate reader (Thermo Fisher Scientific, Waltham, MA, EE. UU).

Methods

Preparation and formation of PLGA NPs control and encapsulated with OBE100

The EEM method was used to encapsulate OBE100 in PLGA NPs (50:50) under the conditions described by Escobar et al. (2023). Initially, two phases were obtained, aqueous and organic (W/O). In the organic phase, 80 mg of PLGA 50:50 was dissolved in 4 mL of ethyl acetate and sonicated in an ultrasonic bath for 1 min. OBE100 (16 mg) was then added, and the sonication cycle was repeated. This was followed by addition of tocopherol solution (1 mL) and the mixture was sonicated for 1 min. After mixing the organic phase, 8 mL of the aqueous phase of kolliphor was added and a new sonication cycle was performed for 3 min to obtain a homogeneous mixture. The obtained nanoemulsion was subjected to pulses in a UP100H Herschel ultrasonic equipment using a 0.5-inch probe to prepare the nanoemulsion by pulses at different amplitudes and sonication times. Table I lists the acronyms used for the PLGA 50:50 NPs without (A_C) and encapsulated (A_E) OBE100, where the first two numbers correspond to the sonication time (5.0, 7.5, and 10 min) and the last two numbers are the amplitudes used in sonication (20, 30, 40%, and 60%). The emulsification process was followed by evaporation of the organic solvent through continuous stirring at 400 rpm.

Determination of optimal conditions for OBE100 nanoencapsulation

Once the amplitude and sonication time for the encapsulation of A_C and A_E NPs were standardized under the conditions established by Escobar et al. (2023), three new formulations were established by varying the PLGA: OBE100 ratio (60:12, 80:16, and 100:20), with their respective controls without encapsulation. Equal volumes of ethyl acetate, kolliphor, and tocopherol were used in the previous section to determine how the concentration of OBE100 affects the encapsulation process.

Table II shows the final process conditions with their respective acronyms, where A is defined above; letter C refers to the control (without OBE100); letter E is NPs encapsulated

Table I. Formulations used in the standardization of NPs Ac and A_E.

Samples	Time (min)	Amplitude (%)	Samples	Time (min)	Amplitude (%)
A_C5.020	5	20	A_E5.020	5.0	20
A_C7.520	7.5	20	A_E7.520	7.5	20
A_C1020	10	20	A_E1020	10	20
A_C5.030	5	30	A_E5.030	5.0	30
A_C7.530	7.5	30	A_E7.530	7.5	30
A_C1030	10	30	A_E1030	10	30
A_C5.040	5	40	A_E5.040	5.0	40
A_C7.540	7.5	40	A_E7.540	7.5	40
A_C1040	10	40	A_E1040	10	40
A_C5.060	5	60	A_E5.060	5.0	60
A_C7.560	7.5	60	A_E7.560	7.5	60
A_C1060	10	60	A_E1060	10	60

with OBE100; the first two (60 and 80) or three numbers (100) after the letters C or E refer to the PLGA ratio; and the last two numbers are the amounts of OBE100 used in the preparation of NPs (12, 16, and 20 mg).

Dynamic light scattering (DLS)

This analysis allowed for the determination of the particle size (nm), polydispersity index (PDI), and Zeta potential (PZ) (mV) of all NPs obtained in the present study. It was performed using a Malvern Instruments Zetasizer NS instrument with an incidence angle of 173° and wavelength of 633 nm. The samples were prepared in solutions containing 100 µL of the dispersion and 900 µL of Type II water. Each measurement was performed in triplicates.

Purification and lyophilization of nanoemulsions

Purifying A_E6012, A_E8016, and A_E10020 NPs and their respective controls were performed using 20 cm cellulose membranes (M_W: 12-14 kDa) hydrated in type II water for 15 min before use. Dialysis was used as a washing and purification medium to extract all non-particulate compounds. Subsequently, the samples were lyophilized in a Labconco® lyophilizer under the following conditions: vacuum 0.1 mbar, time 12 h, and temperature -60°C. The volume used was 300 mL.

Table II. Standardized process conditions to obtain A_C and A_E NPs.

Samples	PLGA (mg)	OBE100 (mg)
A_C60	60	-
A_E6012	60	12
A_C80	80	-
A_E8016	80	16
A_C100	100	-
A_E10020	100	20

A_C: PLGA control without OBE100, A_E: PLGA encapsulated with OBE100.

Loading capacity (LC) and EE

The amount of encapsulated OBE100 was reported as the total content of its three major components: UAL, OA, and UA. For this purpose, 7–8 mg of AE6012, AE8016, and AE10020 NPs were dissolved in 1 mL of methanol, and the mixture was sonicated for 20 min at 35°C. Subsequently, the samples were centrifuged at 10000 rpm for 20 minutes. Finally, the mixture was filtered through 0.25 µm syringe filters, and high-performance liquid chromatography (HPLC) was used to quantify the amount of released extract. The equations used for the determination of LC (Equation 1) and EE (Equation 2) were as follows (Mejía et al. 2021):

$$LC\ (\%) = \frac{H}{I}\ x\ 100 \quad (1)$$

$$EE\ (\%) = \frac{J}{K}\ x\ 100 \quad (2)$$

Where H, I, *J*, and *K* are the masses of the OBE100 encapsulated, the mass of the PLGA NPs, and total OBE100 in the supernatant, respectively, and K is the total OBE100 used for encapsulation.

Evaluation of in vitro cell viability of PLGA NPs encapsulated with OBE100 cell cultures

-Myotubes cell culture C2C12

The C2C12 CRL-1772™ cell line was cultured in 75 mL flasks at 37°C and 5% CO_2, in Dulbecco's modified Eagle medium (DMEM) enriched with 25 mM glucose and 10% fetal bovine serum (FBS) every two days until 80% confluence was reached. Differentiation medium (DMEM + 25 mM glucose + 2% FBS) was added and incubated for 5–7 days, with medium changes every two days, until differentiation into myotubes. Subsequently, OBE100 encapsulated (A_E6012,

A_E8016, and A_E10020) and non-encapsulated (A_C100) PLGA NPs dissolved in DMEM were added and incubated for 4 h to assess the viability.

-Adipocyte cell culture 3T3-L1

3T3-L1 CL-173™ cell line were cultured at 37°C and 5% CO_2, with medium changes (DMEM + 25 mM glucose + 10% FBS) every two days until 80% confluence was reached. Differentiation medium 1 (DMEM, 25 mM glucose, 10% FBS, 1 µg/mL insulin, 0.25 µM dexamethasone, 0.5 mM 3-Isobutyl-1-methylxanthine (IBMX), and 2 µM rosiglitazone) was added and incubated for 48 h, followed by a switch to differentiation medium 2 (DMEM, 25 mM glucose, 10% FBS, 1 µg/mL insulin) for another 48 h. Once differentiated into adipocytes, PLGA NPs were encapsulated with OBE100 (A_E6012, A_E8016, and A_E10020) and unencapsulated (A_C100) dissolved in differentiation medium 1 and incubated for 6 days, with medium changes every two days. The culture medium was removed at the end of the treatment, and cell viability was evaluated.

-Hepatocyte cell culture HepG2

The human hepatocyte cell line HepG2 HB-8065™ was maintained at 37°C and 5% CO_2, renewing the medium (DMEM + 5.5 mM Glucose + 10% FBS) every two days until 80% confluence was reached. Fatty acid-loading medium (DMEM, 5.5 mM glucose, 1% bovine serum albumin, 0.333 mM sodium oleate, and 0.167 mM sodium palmitate) was added and incubated for 48 h. Then, OBE100 encapsulated (A_E6012, A_E8016, and A_E10020) and non-encapsulated (A_C100) PLGA NPs dissolved in the medium were added and incubated for 5 days with the medium, and treatment was changed every other day. Once the exposure time to NPs was complete, the culture medium was removed and viability was assessed.

-Macrophage cell culture J774A.1

The J774A.1 HB- TIB-67™ cell line was cultured at 37°C and 5% CO_2, with medium changes (DMEM + 25 mM glucose + 10% filtered FBS) every two days until 80% confluence. Differentiation medium 1 (DMEM, 25 mM glucose, 10 ng/mL lipopolysaccharide, and 20 ng/mL interferon γ) was added and the cells were incubated for 18 h. Subsequently, OBE100-encapsulated (A_E6012, A_E8016, and A_E10020) and non-encapsulated (A_C100) PLGA NPs solubilized in differentiation medium 1 were incorporated and incubated for 6 h before the viability assessment.

Evaluation of cell viability

The viability of cells exposed to OBE100-encapsulated (A_E6012, A_E8016, and A_E10020), non-encapsulated (A_C100), OBE100-encapsulated, and non-encapsulated (A_C100) NPs were assessed using an MTT assay. C2C12, 3T3-L1, HepG2, and J774.A1 cell lines were treated with various concentrations of NPs (100, 200, 400, and 600 µg/mL). After incubation, the culture medium was removed, the MTT reagent was added, and the cells were incubated for 2 h. DMSO was added to dissolve the formazan crystals, and after dissolution, the absorbance was measured at 570 nm using a Varioskan™ LUX microplate reader. The tests were performed in triplicates. The percentage viability was calculated considering untreated control cells with a value of 100%, using Equation 3:

$$\%\ of\ viability = S\_C\ x100 \quad (3)$$

S corresponds to the absorbance of C2C12, 3T3-L1, HepG2, and J774.A1 cell lines treated with PLGA NPs and C corresponds to control cells not exposed to PLGA NPs.

This study established that nanoformulations with less than 70% viability are cytotoxic according to ISO 10993-5: Biological

evaluation of medical devices, Part 5: *In vitro* cytotoxicity tests (ISO 2009).

Statistical analysis and design of experiments

The results obtained in preparing and forming PLGA NPs of A_E and A_C and evaluating the cell viability of C2C12, 3T3-L1, HepG2, and J774.A1 cell lines are presented as mean ± standard deviation (SD). Between-group comparisons were performed using analysis of variance (ANOVA), followed by Dunnett's post-hoc test, assuming equal variances with minimum significant differences (LSD). Statistical analyses were performed using SPSS Statistics 27.0.1 software.

For the optimization of A_E6012, A_E8016, and A_E10020 NPs, experiments were designed using the method of surface response (MSR) of multiple comparisons performed using the statistical software Minitab, with a significance level of ($P < 0.05$). The factors evaluated were the amounts of PLGA 50:50 (mg) and OBE100 (mg). The response variables evaluated were the particle size, PDI, PZ, EE (%), and LC (%). Coded data were used to simplify the calculations and analyses. The coded data were transformed so that the independent variables had values within a standard range, such as (-1.1). Each independent variable was assigned a minimum or maximum value (Table III).

RESULTS AND DISCUSSION

Optimization of amplitude and time conditions for the encapsulation process of OBE100 extract in PLGA NPs

The particle size distributions of the control and OBE100-encapsulated samples at different sonication times (5.0, 7.5, and 10 min) using amplitudes of 20, 30, 40, and 60% are shown in Figure 1. Samples prepared at an amplitude of 20% presented mainly polymodal behaviour, as only sample A_C5.020 exhibited monomodal behaviour (Figure 1a, b). Among the A_C samples (Figure 1c), only A_C5.030 exhibited a polymodal distribution for the samples obtained using a 30% amplitude (Figures 1c, d). However, in the A_E samples (Figure 1d), the same distribution was observed for A_E5.030 and A_E7.530.

All the AC samples obtained at 40% amplitude (Figure 1e) exhibited a monomodal distribution. However, among the A_E samples prepared at the same amplitude (Figure 1f), this distribution was only observed for A_E7.540. All the A_C and A_E samples obtained at an amplitude of 60% presented a monomodal distribution (Figure 1g, h). The polymodal behaviour exhibited by some samples in terms of size, PDI, and PZ was possibly due to the different distributions of OBE100 in these NPs, the interaction between OBE100 and PLGA. Also, the migration of some OBE100 components from the particles to the aqueous phase of small droplets of OBE100,

Table III. Conversion from coded to uncoded units for PLGA and OBE100.

Level	Factor 1		Factor 2	
	A: PLGA (mg)		B: OBE100 (mg)	
	Coded units	Uncoded units	Coded units	Uncoded units
Minimum	-1	60	-1	12
	-0.5	70	-0.5	14
Medium	0	80	0	16
Maximun	0.5	90	0.5	18
	1	100	1	20

which were dispersed in the aqueous phase (Escobar et al. 2023).

Tables IV and V list the particle sizes, PDI, and PZ of the A_C and A_E samples prepared at different amplitudes and times. The encapsulated NPs (Table V) showed an increase in particle size ($P < 0.05$), indicating the encapsulation of OBE100. The same behaviour was observed for the encapsulation of UA in dendrimer NPs (Alfei et al. 2021) and PLGA NPs encapsulated with antibiotics (Gaspar et al. 2018). Therefore, the particle sizes of the A_E NPs are larger than those of the A_C samples prepared under the same conditions (Tables IV and V).

The A_C samples exhibited smaller particle sizes than those of the A_E samples ($P < 0.05$). In addition, no trend was observed in particle size with time; however, at 10 min and 60% amplitude, the smallest particle sizes were obtained for the A_C and A_E samples ($P < 0.05$). However, in the case of PDI values of the A_C samples, no significant differences were observed from those of the A_E

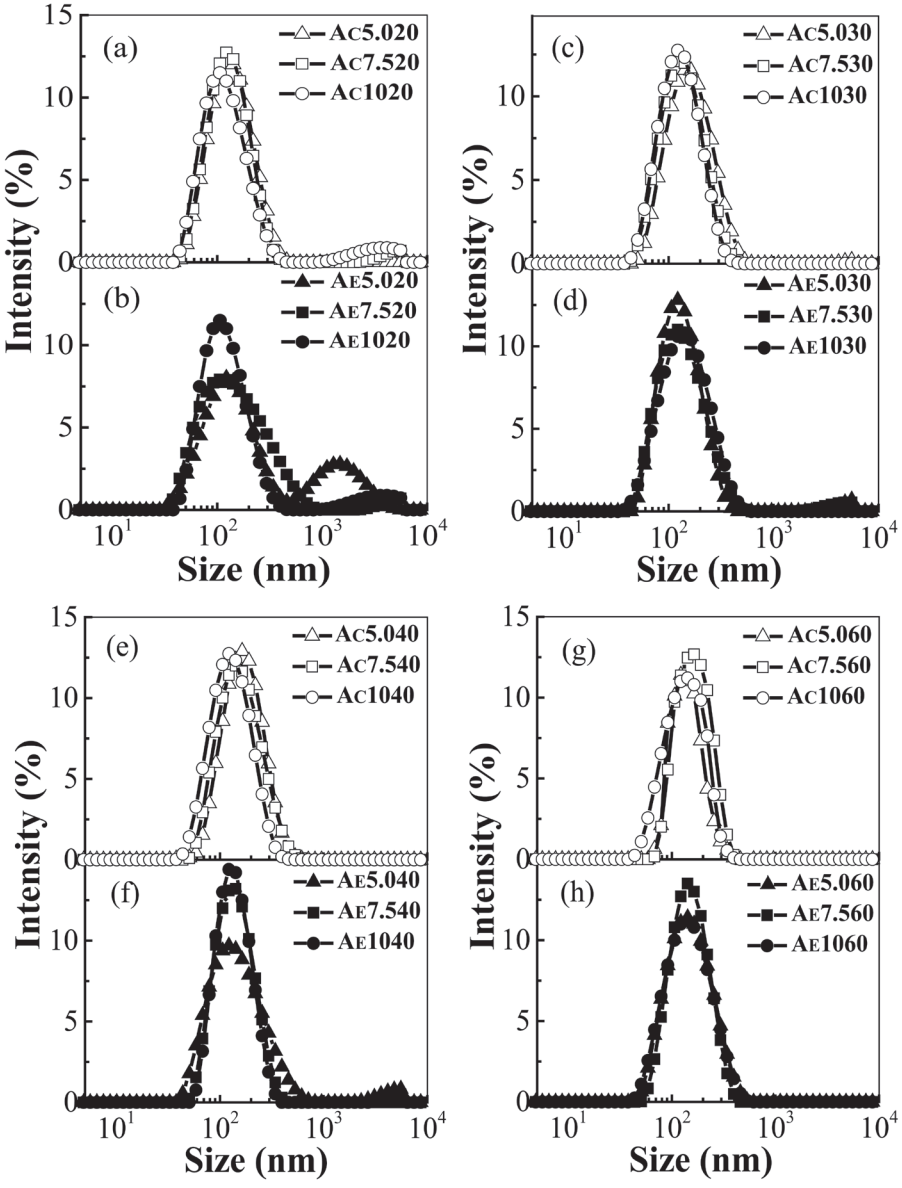

Figure 1. Size distribution of NPs without OBE100 (A_C) and those encapsulated in OBE100 (A_E) at different sonication times (5.0, 7.5, and 10 min) and amplitudes of 20% (a and b), 30% (c and d), 40% (e and f), and 60% (g and h).

samples, nor was there a trend with time and amplitude ($P < 0.05$). The PDI value of NPs was < 0.3. Therefore, all systems were moderately polydisperse (Sánchez et al. 2020).

The different behaviors observed in particle sizes of the samples (A_C and A_E) were due to factors such as sonication time, amplitude, M_w, viscosity, PLGA ratio, amount of OBE100, PLGA-OBE100 interactions, tocopherol or kolliphor absorption or desorption, and tocopherol and kolliphor desorption (Mendoza et al. 2016, Ruiz et al. 2022, Wischke & Schwendeman 2008). However, nanoencapsulation of OBE100 was performed in all the cases. The samples prepared at an amplitude of 60% exhibited the smallest particle sizes, which was attributed to the higher cavitation caused by sonication (Ruiz et al. 2022). The particle sizes depended on the amplitude and time used but did not show a trend in these parameters (Tables IV and V). This was possibly due to different interactions between the components and migration of kolliphor and/or tocopherol to the aqueous phase.

The A_C samples with the lowest PDI values ($P < 0.05$) were A_C7.560, A_C1060, and A_C1040, respectively. This indicates that time and amplitude influence PDI under these conditions. This behaviour is likely due to lower resistance to the cavitation process, thus producing more monodisperse NPs.

The negative PZ values were mainly due to the presence of AU on the surface of the NPs (Alfei et al. 2021), as kolliphor is a nonionic block

Table IV. The particle size, PDI, and PZ of the Ac NPs were presented as amplitude functions.

Acronym	Factors		Response variables		
	Treatments		Size (nm) ± SD	PDI ± SD	PZ (mV) ± SD
	Time (min)	Amplitude (%)			
A_C5.020	5	20	123.906 ± 3.426[a]	0.281 ± 0.043[a]	-30.933 ± 0.986[a]
A_C7.520	7.5	20	121.693 ± 1.387[a]	0.264 ± 0.022[a]	-27.833 ± 1.159[b]
A_C1020	10	20	118.596 ± 0.433[b]	0.232 ± 0.012[a]	-29.266 ± 1.242[b]
	P-value		0.061	0.199	0.042
A_C5.030	5	30	118.533 ± 0.321[a]	0.238 ± 0.046[a]	-34.466 ± 3.419[a]
A_C7.530	7.5	30	119.206 ± 1.008[a]	0.204 ± 0.025[a]	-34.466 ± 0.351[a]
A_C1030	10	30	117.900 ± 0.300[a]	0.210 ± 0.012[a]	-32.900 ± 0.458[a]
	P-value		0.115	0.413	0.573
A_C5.040	5	40	117.786 ± 0.673[a]	0.255 ± 0.013[a]	-35.933 ± 1.159[a]
A_C7.540	7.5	40	117.406 ± 0.390[a]	0.254 ± 0.029[a]	-36.233 ± 0.450[a]
A_C1040	10	40	116.833 ± 0.550[a]	0.157 ± 0.008[b]	-35.933 ± 0.757[a]
	P-value		0.183	0.001	0.883
A_C5.060	5	60	110.166 ± 0.321[a]	0.186 ± 0.007[a]	-33.266 ± 0.416[a]
A_C7.560	7.5	60	109.300 ± 0.964[a]	0.185 ± 0.010[a]	-34.333 ± 0.971[a]
A_C1060	10	60	107.966 ± 0.404[b]	0.172 ± 0.005[a]	-34.133 ± 0.493[a]
	P-value		0.015	0.133	0.2

Different letters in the columns indicate the minimum significant differences according to the DMS-ANOVA test ($P < 0.05$) between the treatments for each process stage. SD=standard deviation. n=3. A_C: PLGA without OBE100, A_E: PLGA encapsulated with OBE100.

copolymer (polyoxyethylene-polyoxypropylene) (Yurtdaş-Kırımlıoğlu 2022). However, it has also been reported that this can be attributed to the formation of carboxylate groups on the NPs due to PLGA hydrolysis. (Jo et al. 2020). The PZ of the A_C samples (Table IV) did not show a trend with the applied amplitude or time, but showed good stability, as the PZ presented more negative values. The A_E samples did not exhibit significant differences in PZ ($P > 0.05$) from those of the A_C obtained under the same time and amplitude conditions.

The sizes of the NPs of the A_C samples were smaller than those reported for PLGA NPs, whose sizes were 132.8 ± 1.5 nm (PLGA 75:25, M_w between 10 and 20 kDa) (Lu et al. 2019), 147.5 ± 1.48 nm, (PLGA 50:50, M_w:17 kDa) (Hu et al. 2019), 150 ± 0.02 nm (PLGA 50:50 M_w: 24-38 kDa) (Escobar et al. 2023) and 339.1 ± 14.36 nm (PLGA 50:50, M_w:12-20 kDa) (Sanapalli et al. 2023).

The NPs sizes of the A_E samples were smaller than those reported for PLGA 50:50 NPs encapsulated with 17-Dimethylaminoethylamino-17-Demethoxygeldanamycin (between 305.5 and 489 nm) (Cruz et al. 2021). The latter sample had a PDI value of 0.19 ± 0.02 and a PZ of -38 mV (Escobar et al. 2023). The difference between the latter results and those obtained in the present study is attributed to the M_w of the PLGA used (24-38 kDa) (Escobar et al. 2023).

The PDI values of the A_C samples are comparable with those reported for PLGA 50:50 and PLGA 75:25 NPs, whose values were, respectively, 0.256 ± 0.012 (Hu et al. 2019) and

Table V. The particle size, PDI, and PZ of the A_E NPs are presented as functions of the amplitude.

Samples	Factors		Response variables		
	Treatments		Size (nm) ± SD	PDI ± SD	PZ (mV) ± SD
	Time (min)	Amplitude (%)			
A_E5.020	5	20	149.933 ± 1.436[a]	0.416 ± 0.008[a]	-23.333 ± 0.763[a]
A_E 7.520	7.5	20	144.766 ± 3.917[a]	0.315 ± 0.034[b]	-23.733 ± 0.416[a]
A_E 7.520	10	20	134.823 ± 4.263[b]	0.249 ± 0.007[b]	-30.200 ± 1.752[b]
	P-value		0.005	0	0
A_E 5.030	5	30	136.333 ± 9.960[a]	0.199 ± 0.010[a]	-22.800 ± 0.916[a]
A_E 7.530	7.5	30	143.000 ± 2.551[a]	0.222 ± 0.004[b]	-25.233 ± 0.208[a]
A_E 1030	10	30	136.936 ± 1.504[a]	0.221 ± 0.004[b]	-30.633 ± 0.709[b]
	P-value		0.382	0.012	0
A_E 5.040	5	40	138.716 ± 0.860[a]	0.279 ± 0.023[a]	-29.333 ± 6.007[a]
A_E 7.540	7.5	40	135.866 ± 4.669[a]	0.175 ± 0.013[b]	-24.700 ± 1.322[a]
A_E 1040	10	40	133.733 ± 3.085[a]	0.190 ± 0.021[b]	-32.133 ± 0.611[a]
	P-value		0.251	0.001	0.107
A_E 5,060	5	60	129.000 ± 1.135[a]	0.185 ± 0.047[a]	-32.833 ± 0.873[a]
A_E 7.560	7.5	60	128.466 ± 0.288[a]	0.169 ± 0.018[a]	-31.633 ± 0.950[a]
A_E 1060	10	60	124.766 ± 4.266[a]	0.171 ± 0.010[a]	-31.733 ± 1.331[a]
	P-value		0.167	0.781	0.375

Different letters in the columns indicate the minimum significant differences according to the DMS-ANOVA test ($P < 0.05$) between the treatments for each process stage. SD=standard deviation. n=3. A_C: PLGA without OBE100, A_E: PLGA encapsulated with OBE100.

0.155 ± 0.03 nm (Lu et al. 2019). These were lower than those reported for the PLGA 50:50 M_w: 24-38 kDa, whose values were 0.12 ± 0.02 nm (Mejía et al. 2021) and 0.14 ± 0.01 nm (Escobar et al. 2023). In addition, some PZ values of the NPs of the A_C samples obtained in this study (Table IV) were comparable with that reported by Hu et al. (2019) for PLGA NPs 50:50 (-25.93 ± 0.58 mV) (Hu et al. 2019). These were lower than that reported by Escobar et al. (2023) for PLGA 50:50 (-43 mV) (Escobar et al. 2023), but higher than those reported by Vicari et al. (2008) for PLGA 50:50 (M_w: 7-17 kDa) whose values were between -5.20 ± 0.10 and 4.60 ± 0.20 mV (Vicari et al. 2008).

Considering that the PDI values of the samples prepared with 60% amplitude (A_E7.560 and A_E1060) were similar (P > 0.05) (Table V). The other encapsulated NPs were obtained using 60% amplitude and 7.5 min time but varying the concentrations of PLGA and OBE100.

Determination of the optimal PLGA: OBE100 ratios to obtain the lowest PDI and highest stability of NPs encapsulated with OBE100

The optimal ratio of PLGA to OBE100 needed to obtain the lowest PDI and the highest stability of NPs were determined. Figure 2 shows the particle-size distributions of the control sample (Figure 2a) and OBE100-encapsulated samples (Figure 2b). For the control samples of NPs obtained with A_C, except for sample A_C6012, all the distributions were monomodal. Among the samples of this polymer encapsulated in OBE100, only A_E8016 exhibited monomodal distribution.

Table VI presents the particle size, PDI, and PZ values of the control and OBE100-encapsulated samples for the optimized PLGA NPs. All the encapsulated samples had larger particle sizes than the control sample indicating therefore, that OBE100 was encapsulated in the PLGA NPs. The highest variability in particle size (difference between the particle sizes of the encapsulated

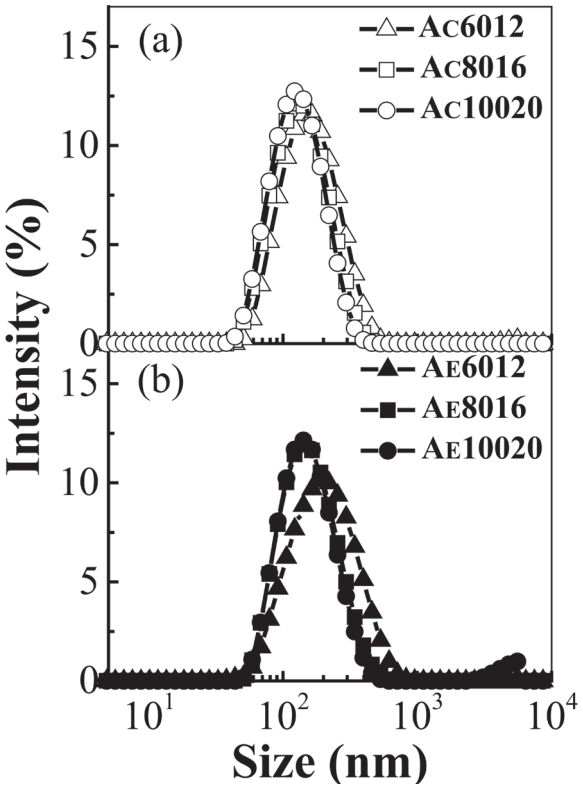

Figure 2. Size distribution of NPs without OBE100 (A_C) and encapsulated with OBE100 (A_E), with previously established amplitude and time conditions based on the ratios of PLGA (60, 80, 100) mg:OBE100 (12, 16, 20) mg. (a) Control NPs of A_C 6012, A_C 8016, and A_C 10020 (b) Encapsulated NPs of A_E6012, A_E8016, and A_E10020.

and control samples) was approximately 31 nm (A_E6012). This indicated that this sample had the highest OBE100 content. However, this will further be elucidated using LC and EE results.

It is essential to highlight that in all cases, the same ratio of PLGA to OBE100 was used. The differences in the particle size results were mainly attributed to the amount of PLGA and OBE100 used in each case, cavitation caused by the application of ultrasound and cavitation caused by the application of ultrasound (Ruiz et al. 2022). Additionally, the migration of OBE100 into the dispersion medium (Alirezaei et al. 2022), and interaction between PLGA and OBE100 (Liu et al. 2021). This is also the reason for the absence of a trend in particle size with increasing

Table VI. Particle size, PDI, and PZ of A_C and A_E samples.

Acronyms	Factors		Response variables		
	Treatments		Size (nm) ± SD	PDI ±SD	PZ (mV) ± SD
	PLGA (mg)	OBE100 (mg)			
A_C6012	60	12	143.533 ± 1.625[a]	0.189 ± 0.009[a]	-23.800 ± 0.264[a]
A_C8016	80	16	122.233 ± 1.700[b]	0.159 ± 0.012[b]	-36.866 ± 0.737[b]
A_C10020	100	20	116.000 ± 0.655[b]	0.143 ± 0.024[b]	-31.133 ± 0.585[b]
P-value			0	0.041	0
A_E6012	60	12	174.900 ± 1.539[a]	0.218 ± 0.009[a]	-25.900 ± 0.700[a]
A_E8016	80	16	141.800 ± 1.058[b]	0.177 ± 0.013[b]	-34.800 ± 1.352[b]
A_E10020	100	20	143.833 ± 1.078[b]	0.219 ± 0.005[a]	-33.500 ± 0.721[b]
P-value			0	0.003	0

Different letters in the columns indicate the minimum significant differences according to the DMS-ANOVA test (P < 0.05) between the treatments for each process stage. SD=standard deviation. n=3. A_C: PLGA without OBE100, A_E: PLGA encapsulated with OBE100.

amounts of PLGA and OBE100 (P > 0.05). Another important aspect was that with increasing PLGA amounts, the size of the NPs increased. This has been reported for other drugs (prodigiosin and paclitaxel) encapsulated in PLGA-polyethylene glycol NPs. However, this did not occur, possibly because of the plasticizing effect of the OBE100 components (Jusu et al. 2020). All PDI values (Table VI) were less than 0.3 indicating moderately polydisperse systems (Sánchez et al. 2020), and in some cases, the values of the control and the encapsulated samples were similar. No trend was observed in the PDI with PLGA content or with the amount of OBE100, possibly because of interfacial phenomena or the interaction between the PLGA and OBE100 components.

In the case of the encapsulated samples, only the PZ of the A_E6012 samples showed higher values of -30 mV, thus, it had the lowest colloidal stability (Alfei et al. 2021, Ruiz et al. 2022). However, as in the case of PDI, no trend was observed for the PLGA and OBE100 amounts.

All NPs had sizes between 100 and 200 nm, which is a relevant result because particles of these sizes have been reported to be easily removed from the blood by the reticuloendothelial system after releasing the active principle (Sun et al. 2019). In addition, NPs with small sizes have shorter circulation times than NPs with large sizes (> 200 nm), and are easily phagocytosed (Sun et al. 2019). Optimization of the PLGA NPs preparation conditions allowed the preparation of OBE100-encapsulated PLGA NPs with small particle sizes and PDI, which are suitable for controlled drug release. Furthermore, considering that kolliphor is a nonionic surfactant, the system is considered electrosterically stable (Ruiz et al. 2022).

The particle size values of some of the samples (Table VI) are comparable to those of PLGA NPs.50:50 of M_w: 17 kDa, M_w: 15-25 kDa and M_w: 24-38 kDa encapsulated with astasanthin (between 146.40 and 369.27 nm) (Hu et al. 2019), ádeoxyribonucleic acid (160 nm) (Jo et al. 2020) and OBE100 (168 ± 0.01 nm) (Escobar et al. 2023), respectively. The PDI and PZ values reported for NPs encapsulated with deoxyribonucleic acid and OBE100 were 0.11 and -33 mV (Jo et al. 2020), and 0.19 and -38 mV (Escobar et al. 2023)

respectively. These values are comparable with some of those obtained in the present study (Table VI).

LC and EE

Assessment of the LC and EE for the A_E NPs with OBE100 samples were conducted, and the results summarized in Table VII. Sample A_E10020 showed a higher LC value than other samples obtained with PLGA NPs, whereas sample A_E6012 showed the highest EE value. This indicates that under the preparation conditions and composition used for this sample, there was more significant interaction between the PLGA NPs and the OBE100 components, resulting into low migration of OBE100 into the aqueous phase (Arınmış et al. 2024). Notably, an EE value of 81.57% is considered high and suitable for oral drug administration (Arınmış et al. 2024).

The LC and EE values of A_E were lower than those reported by Escobar et al. (2023) for OBE100 encapsulated in PLGA NPs (50:50, M_w: 24-38 kDa), which were 6.4% and 92 %, respectively (Escobar et al. 2023). This behaviour was associated with the difference in M_w of the polymers. The EE values of the present study are higher than those reported for PLGA NPs (Resomer RG 503H 50:50) encapsulated with 17-dimethylaminoethylamino-17-demethoxygeldanamycin (between 14.9-17%) (Cruz et al. 2021) and with ferulic acid (76.48 ± 3.12%) (Arınmış et al. 2024). The EE values of samples A_E6012 and A_E10020 are much higher than those of PLGA NPs (50:50, M_w: 4-15 kDa) encapsulated with apremilast (between 39.5 ± 1.1 and 61.1 ± 1.9%) (Anwer et al. 2019). These results allowed us to conclude that A_E6012 and A_E10020 presented the best encapsulation results (higher LC and EE values). Therefore, these samples were further evaluated using MSR statistical designs to determine the optimal operating conditions to achieve maximum efficacy with minimal side effects.

The LC and EE values of A_E were lower than those reported by Escobar et al. (2023) for OBE100 encapsulated in PLGA NPs (50:50,

Table VII. EE and LC values of A_E NPs.

Acronyms	Components	LC (%) ± SD	EE (%) ± SD
A_E6012	UAL	0.192 ± 0.036	76.830 ± 14.246
	OA	0.302 ± 0.011	81.583 ± 2.867
	UA	1.391 ± 0.015	82.268 ± 0.893
	OBE100	1.885 ± 0.042[a]	81.569 ± 1.798[a]
A_E8016	UAL	0.179 ± 0.034	37.310 ± 7.134
	OA	0.922 ± 0.006	41.061 ± 0.803
	UA	1.390 ± 0.039	42.906 ± 1.200
	OBE100	1.861 ± 0.040[b]	42.004 ± 0.904[b]
A_E10020	UAL	0.249 ± 0.014	80.689 ± 4.679
	OA	0.354 ± 0.014	77.636 ± 3.165
	UA	1.650 ± 0.055	79.257 ± 2.625
	OBE100	2.253 ± 0.082[c]	79.152 ± 2.894[a]
	P-value	0	0

Letters in the columns indicate minimum significant differences according to the DMS-ANOVA test (P < 0.05) between the treatments for each process stage. SD=standard deviation. n=3.

M_w: 24-38 kDa), which were 6.4% and 92 %, respectively (Escobar et al. 2023). This behaviour was associated with the difference in M_w of the polymers. The EE values of the present study are higher than those reported for PLGA NPs (Resomer RG 503H 50:50) encapsulated with 17-dimethylaminoethylamino-17-demethoxygeldanamycin (between 14.9-17%) (Cruz et al. 2021) and with ferulic acid (76.48 ± 3.12%) (Arınmış et al. 2024). The EE values of samples A_E6012 and A_E10020 are much higher than those of PLGA NPs (50:50, M_w: 4-15 kDa) encapsulated with apremilast (between 39.5 ± 1.1 and 61.1 ± 1.9%) (Anwer et al. 2019). These results allowed us to conclude that A_E6012 and A_E10020 presented the best encapsulation results (higher LC and EE values). Therefore, these samples were further evaluated using MSR statistical designs to determine the optimal operating conditions to achieve maximum efficacy with minimal side effects.

Response surface methodology

The response variables evaluated were the size, PDI, PZ, LC, and EE. Nine experimental treatments were performed, with five levels and two factors. This was conducted to evaluate the optimization obtained for the two independent variables PLGA (mg) and OBE100 (mg). Table VIII shows the results of the experimental treatments for the size, PDI, PZ, PZ, LC, and EE. Each response variable (encapsulated NPs) was compared using the MSR linear regression model, with statistical parameter values determined using the Minitab program. The parameters included degrees of freedom (DF), sum of squares (SS), mean square (MS), Fisher value (F-value), P-value, multiple correlation coefficients (R^2), adjusted R^2, and predicted R^2.

Effect of factors on particle size

ANOVA used for the multiple linear regression model in size (Table VIII) showed that the particle size was significant for NPs encapsulated with this polymer, since the F value was 665.61 and the value ($P < 0.05$). In contrast, the R^2 value for this system was 0.9955, indicating that this model could explain 99.55% of the variability in the particle size. The same trend was observed for adjusted R^2 values. The linear equation (Equation 4) for the coded values is as follows.

$$\textit{Size}\ (\textit{nm}) = 141.800 - 15.533X + 17.567XY \quad (4)$$

The regression equation (Equation 4) represents the linear effect of PLGA (X) and OBE100 (Y) on the particle size and the interactive term X*Y, which symbolizes the nonlinear relationship with the response (particle size). The intercept value was 141.800 nm and the expected values of the response variable when the independent variables X and X*Y interactions were zero. Coefficient X indicates an inverse relationship between X and the particle size. The particle size (nm) decreased by 15.533 nm for every unit increase in X, indicating that the X*Y interaction remained constant. In contrast, the X*Y coefficient was positive, indicating that the interaction between X and Y directly affected the particle size. For each unit increase in the products of X (PLGA) and Y (OBE100), the particle size increased by 17.567 nm. Therefore, the multiple linear regression equation indicates that although X has a reducing effect, the combination of X and Y (through their interaction) can counteract this effect and increase particle size (Equation 4). This is related to the results obtained by Govardhane & Shende (2024), who found that the encapsulation of zinc with phthalocyanine in PLGA-chitosan NPs showed that a higher concentration of PLGA together with chitosan produced larger particle sizes. This was ascribed to an increase in the viscosity of the system. This was also observed by Adebileje et al. (2017), who encapsulated bovine serum albumin in PLGA NPs and showed that the estimates of

Table VIII. Results of ANOVA statistical analysis of the multiple regression model for A_E6012, A_E8016, and A_E10020 adjusted for particle size, PDI, PZ, LC, and EE.

Response variables	DF	SS	MS	F-value	P-value	R^2	Adjusted R^2	Predicted R^2
Size								
Model	2	2064.88	1032.44	665.61	0	0.9955	0.994	0.9899
Linear	1	1447.71	1447.71	933.34	0			
PLGA	1	1447.71	1447.71	933.34	0			
Interaction two factor (PLGA y OBE100)	1	617.18	617.18	397.89	0			
Error	6	9.31	1.55					
Total	8	2074.19						
PDI								
Model	2	0.003391	0.001695	17.11	0.003	0.8508	0.8011	0.6643
Linear	1	0.000002	0.000002	0.02	0.906			
PLGA	1	0.000002	0.000002	0.02	0.906			
Interaction two factor (PLGA y OBE100)	1	0.003389	0.003389	34.2	0.001			
Error	6	0.000595	0.000099					
Total	8	0.003986						
PZ								
Model	2	138.66	69.33	73.24	0	0.9606	0.9475	0.9115
Linear	1	86.64	86.64	91.52	0			
PLGA	1	86.64	86.64	91.52	0			
Interaction two factor (PLGA y OBE100)	1	52.02	52.02	54.95	0			
Error	6	5.68	0.9467					
Total	8	144.34						
LC								
Model	2	0.28999	0.144995	42.92	0	0.9347	0.9129	0.853
Linear	1	0.20277	0.202768	60.02	0			
PLGA	1	0.20277	0.202768	60.02	0			
Interaction two factor (PLGA y OBE100)	1	0.08722	0.087223	25.82	0.002			
Error	6	0.02027	0.003378					
Total	8	0.31026						
EE								
Model	2	2951.28	1475.64	356.33	0	0.9917	0.9889	0.9812
Linear	1	8.76	8.76	2.12	0.196			
PLGA	1	8.76	8.76	2.12	0.196			
Interaction two factor (PLGA y OBE100)	1	2942.52	2942.52	710.55	0			
Error	6	24.85	4.14					
Total	8	2976.13						

A_C: PLGA without OBE100, A_E: PLGA encapsulated with OBE100.

the statistical effect of PLGA increased with the concentration of serum in the organic phase, thereby increasing the size of the NPs. Jaswir et al. (2019) found that particle size and PDI depended on the manufacturing conditions such as polymer concentration, stirring speed, solvent/non-solvent ratio, and dispersant concentration.

To determine the optimal (maximum) values of the previous model, Figure 3 shows the response surface and contour plots obtained for each of the response variables analyzed. Where a first-order MSR design was created, including only the linear terms of the dependent variables, PLGA and OBE100, and their response variables (size, PDI, PZ, LC, and EE). The response surface plot allowed the visualization of the behavior in the three dimensions of the linear regression equation. This plot is presented in an R3 plane as a hyperplane, visualizing the contour lines in a three-dimensional space (Gutierrez & Salazar 2012). The contour plot is a two-dimensional (2D) projection of the response surface plot, showing the maxima and minima of the two independent variables according to an established color scale. A color gradient from dark red to purple is observed on the surface of the contour plots. The values of the response variables in the

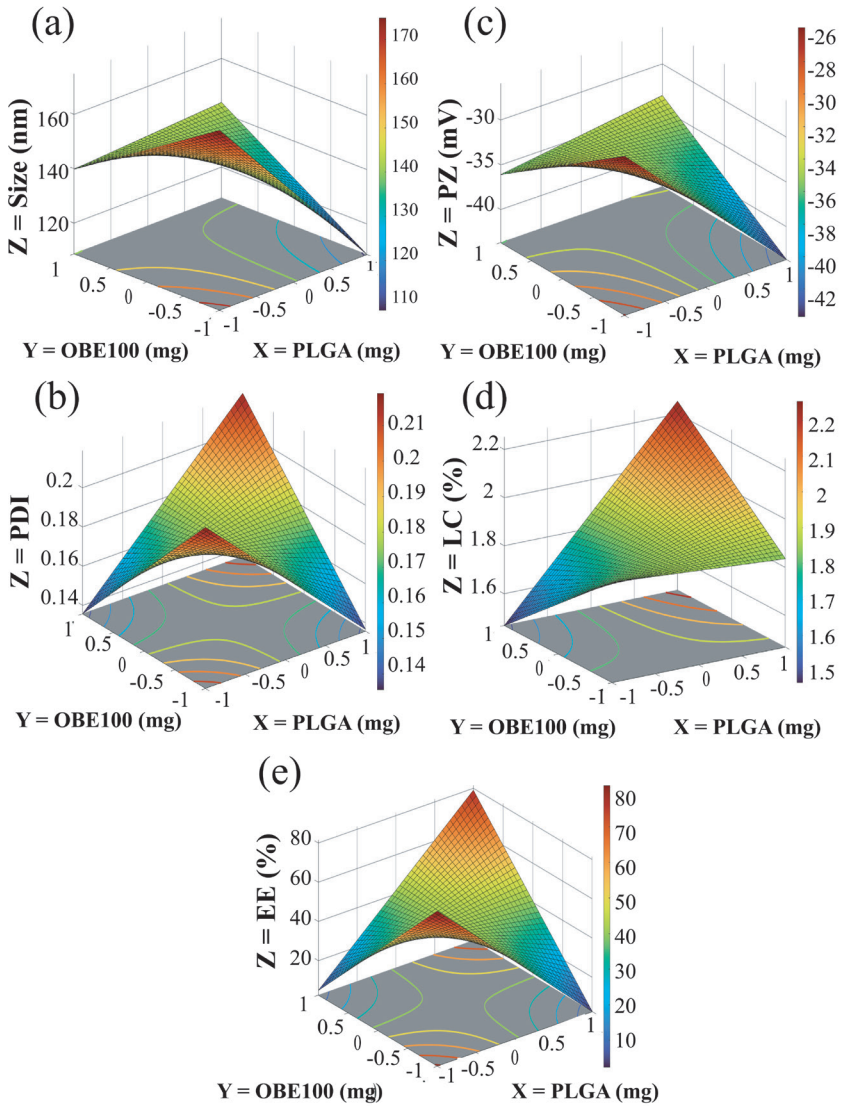

Figure 3. Response surface and contour plots for the encapsulated NPs (AE6012, AE8016, and AE10020) for response variables. a) Size; b) PDI; c) PZ; d) LC and e) EE.

graph are presented on the z-axis, those of PLGA (mg) on the X-axis, and those of OBE100 (mg) on the Y-axis.

For the particle size analysis (Figure 3a), the optimum point was found in the dark red band. The contour plot (lower part of Figure 3a) was characterized by a surface with semi-closed contour lines around the maximum point, approximately 172.10 nm when the coefficient of the PLGA variable was equal to 61 mg and for OBE100 12.27 mg. In both cases, the minimum values for size (nm) would be in the purple color band, opposite to the maximum; the minimum point was 110.07 nm when the proportion of PLGA was 100 mg and OBE100 was 12 mg. This contour plot allowed inferences on the experimental data obtained in this study, demonstrating a similarity in the results of the PLGA NPs size when the PLGA: OBE100 concentration was varied. Therefore, MSR allows visualization of the interactions between two independent variables and how they affect the response variable. This is helpful for the process optimization and the identification of ideal conditions when a specific size and drug potential are required.

Effect of factors on the PDI

The ANOVA results for PDI are presented in Table VIII. The fitted model was highly significant, with a P-value of 0.003 and an F-value of 17.11. The R^2 value for these systems was 0.8508. The suitability of the model for predicting the response in the optimization process was demonstrated, indicating that these models can explain 85.08% of the variability. The same trend was observed for adjusted R^2 values. The regression equation (Equation 5) in coded units is:

$$PDI = 0.17733 + 0.00050X + 0.04117XY \quad (5)$$

Equation 5 shows that the variable X (PLGA) and the interaction between X*Y (PLGA*OBE100) positively affected the PDI. The multiple linear regression equation indicates that although the effect of A alone is minimal, the interaction between X*Y significantly impacts the increase in PDI. Therefore, their combinations significantly affect the variable of interest when the ratio increases.

Figure 3b shows the response surface plot for PDI, which has a slightly curved shape, indicating that both PLGA and OBE100 produced considerable variation in the particle size heterogeneity (Ruiz et al. 2022). Figure 3b shows the maximum value in the dark red shade and minimum value in the purple shade. A contour plot (bottom of Figure 3b) was constructed to obtain the maximum and minimum points. A saddle shape is observed, showing contour lines with hyperbolic shape openings in opposite directions, apparent symmetry, and a point of intersection at the saddle point where the curvature changes. The colour gradient representing the values of the PDI response variable indicated that the maximum values were in the dark red range (approximately 0.2134) when the PLGA coefficient was 98.64 mg and OBE100 coefficient was 19.71 mg. In contrast, the minimum PDI value, 0.1401, was reached when the coefficients of OBE100 and PLGA were 12.18 mg and 99.11 mg, respectively. Based on previous results, it can be considered that the best PDI uniformity in the system would be achieved with the minimum values found. However, a balance of the results should be achieved by contrasting the size-PDI ratio of the NPs.

Effect of factors on the PZ

The ANOVA used for the multiple linear regression model in the PZ is presented in Table VIII, with F value of 73.24 and the value $P < 0.05$. The results indicated that the model terms were significant. In contrast, the R^2 value for the system was 0.9606, indicating that this model could explain

96.06% of the variability in the stability of NPs. The same trend was observed for adjusted R^2 values. The linear equation (Equation 6) in the coded values is:

$$PZ\ (mV) = -34.800 - 3.800X + 5.100XY \quad (6)$$

In multiple regression equation 6, variable X (PLGA) alone has a negative effect on PZ, reducing it. However, the interaction between X*Y (PLGA*OBE100) has a positive effect and can counteract the decrease caused by increasing PZ. This multiple linear regression equation shows how the combined effects of the independent variables and their interactions can influence the response variable. This indicates that a good relationship between the polymer and the active ingredient to be encapsulated is fundamental for standardizing the system and to obtain good results if it is to reach scales for application in humans (Weissig et al. 2014). This was evidenced by the different experiments performed in this study. The PZ remained almost constant and was not affected by the difference in particle size, even though the proportions of PLGA and OBE100 were varied. Therefore, the resulting particles have a larger surface area, exposing more carboxylic acid groups on the surface. However, the surfactant employed or self-assembled on the surface of the NPs may mask the charge associated with the opposing carboxylic groups. This contrasts to the research conducted by Govardhane & Shende (2024), who employed a PLGA-PVA nanosystem with zinc-loaded chitosan and phthalocyanine-loaded chitosan using MSR with a central composite design, where the maximum and minimum PZ values were between -3.8 and 31.5 mV. In the different experiments conducted by Ruiz et al. (2022), the PZ remained constant and was not affected by the difference in particle size. The PZ range of the PLA NPs systems was between -26.0 to -18.0 mV due to the terminal carboxylic groups that are oriented on the surface of the NPs suspension. In such a system, equilibrium is formed between the acid and carboxylate, which generates negative charges on the NPs.

Notably, in both models (Equations 5 and 6), the coefficient of the PLGA*OBE100 interaction was positive. Therefore, increasing the concentration increased the PZ, a relationship already demonstrated by Ho et al. (2015). This indicated that the PZ of the NPs increased with an increase in the CS/PLGA ratio, which could explain the increase in the size of the NPs.

MSR was applied to determine the optimal value for the models, and the results are presented in Figure 3c. A contour plot showing semi-closed contour line curves around the maximum point is shown at the bottom of Figure 3c. A color gradient was observed, representing the response variable PZ (mV). The area for the maximum values of this variable would be in the purple color band, around -43.122 mV, when the coefficient of the PLGA variable was equal to 100 mg and that of OBE100 was 12 mg. The minimum values for PZ would be in the dark red band, opposite to the maximum, that is, approximately -26.62 mV, which was found when the coefficient of the PLGA variable was equal to 61.06 mg and for OBE100, a value of 12.20 mg.

Effect of factors on LC

The ANOVA results for LC are shown in Table VIII. The F value obtained was 42.92 with a value $P < 0.05$. These results indicate the significance of the regression models. However, R^2 determined that the variability of the model explains the LC in 93.47%; that is, it dramatically influences the response variable, in which the regression model (Equation 7) obtained is

$$LC(\%) = 1.8603 + 0.1838X + 0.2088XY \quad (7)$$

Equation 7 shows that both the variable X (PLGA) alone and its interaction with Y (OBE100)

had positive effects on LC (%). This multiple linear regression equation shows how the combined effects of the independent variables and their interactions can influence the LC of NPs. A good fit ($P < 0.05$) and R^2 were obtained by Hu et al. (2019) for the encapsulation of astaxanthin in PLGA NPs. They confirmed its effect and influence when the concentrations of the independent variables (astaxanthin and PLGA) were varied in an MSR model. However, Haider & Soni (2022) investigations of artificial neural networks of phosphatidylserine-targeted nanocarriers for the effective treatment of cancer, established that drug LC did not differ significantly among the obtained NPs. This could be because the drug and polymer in both formulations were present in the same ratio. Ghari et al. (2014) prepared PLGA NPs encapsulated with azithromycin and obtained nanometer monodisperse nanocapsules exhibiting high drug LC as the concentration increased.

MSR was applied to determine the optimal values of the model, and the results are shown in Figure 3d. To determine the maximum values obtained by the LC response variable, a contour plot was obtained (lower part of Figure 3d), where semi-open contour lines were observed and are represented by a dark red gradient whose maximum value for LC was approximately 2.24% when the coefficient of the PLGA variable was equal to 99.63 mg and for OBE100 the value was approximately 19.93 mg. A minimum LC value of 1.47% was observed in the purple band at concentrations of approximately 60 mg for PLGA and 20 mg for OBE100. Therefore, the optimized operating conditions were similar to those obtained experimentally, and the maximum LC values for PLGA NPs were obtained under the same conditions, which were useful and reproducible for further studies.

Effect of factors on EE

The ANOVA results for response variable EE are presented in Table VIII. The F-value and P-value obtained were 356.33 and $P < 0.05$ respectively, indicating great significance for the regression model between EE and independent variables. The variability of the model was explained by an R^2 value of 99.17%, resulting in excellent data fit. In Equation 8, the variable A (PLGA) has an inverse relationship between X and EE. EE decreased by 1.208 percentage units for every one-unit increase in X, whereas its interaction with Y (OBE100) had a positive and significant effect as the OBE100 concentration increased. This multiple linear regression equation shows how the combined effects of the independent variables and their interactions can influence the EE of NPs.

$$EE(\%) = 42.00 - 1.208X + 38.36XY \quad (8)$$

It is noteworthy that the coefficient X had an antagonistic effect when the polymer ratio was varied during optimization. This is opposite to most research reports that employed the MSR in second-order quadratic designs with different concentrations of the active ingredient and PLGA in the NPs because EE is related to the concentration of PLGA present in the NPs. Thus, the higher the PLGA concentration, the higher the EE, which differs from some research reported by Govardhane & Shende (2024), Waghulde et al. (2019). Where they investigated Zinc and phthalocyanine for the treatment of diabetic diseases with a maximum EE of 75% (Govardhane & Shende 2024), and vildagliptina with anti-hyperglycemic activity for the treatment of DM2 with a maximum EE of 76.44% (Waghulde et al. 2019). Although the PLGA coefficient had an antagonistic effect, the results obtained in the present analysis allowed us to obtain a statistically significant ES.

Response surface and contour plots were obtained to determine the maximum and minimum values for the model (Figure 3e). In the contour plot (lower part of Figure 3e), a saddle-shaped surface was obtained, showing hyperbolic contour lines opening in opposite directions, apparent symmetry, and a point of intersection at the saddle point where the curvature changes. The color gradient shows that the area for the maximum values of the response variables is in the dark red band. The maximum value for the variable of interest, EE, was 80%, and was found when the coefficient of the PLGA variable was equal to 60 mg, and for OBE100, a value of 12 mg. In contrast, a minimum EE value of 5.52% was obtained when the coefficient of the PLGA variable was 99.30 mg, and that of OBE100 was 12.18 mg (purple band). Therefore, these optimization results indicated that the maximum values used for the PLGA and OBE100 response variables were acceptable, well-adjusted, and highly reproducible.

Evaluation of cell viability of PLGA NPs encapsulated with OBE100

Cell viability in C2C12

The viability of C2C12 cell line exposed to OBE100-encapsulated (A_E6012, A_E8016, and A_E10020) and non-encapsulated (A_C100) PLGA NPs are presented in Figure 4a. When comparing the results obtained with untreated control cells, statistically significant differences were observed ($P < 0.05$) associated with exposure to A_E6012 treatment at 600 µg/mL. Despite this, the viability in the C2C12 line exposed to both encapsulated and control NPs remained in the range of 73.5 ± 7.7% and 99.47 ± 10%, without affecting the viability of this cell line.

These results are consistent with the findings of Guglielmi et al. (2019), who demonstrated that PLGA NPs encapsulated with pentamidine at concentrations up to 0.4 mg/ml did not exert cytotoxic effects on C2C12 cells. Similarly, Wang et al. (2023) observed that PLGA microspheres encapsulated in metformin only affected the viability of this cell line when undiluted, thereby underlining the biocompatibility of PLGA. Additionally, the absence of a clear correlation between the treatment type, nanoparticle concentration, and percentage viability may reflect experimental variability (Reddin et al. 2023).

Cell viability in 3T3-L1

The viability of 3T3-L1 cell line treated with OBE100-encapsulated (A_E6012, A_E8016, and A_E10020) or non-encapsulated (A_C100) PLGA NPs is shown in Figure 4. There were no statistically significant differences ($P > 0.05$) between the viability of cells treated with NPs and untreated control cells, with viabilities ranging from 81.1 ± 10.25% to 114.3 ± 9.6%. Interestingly, A_E10020 and A_C100 NPs showed viabilities higher than 100%, suggesting two possible causes. First, the treatments may be well tolerated by cells and could even favour cell division (Yan et al. 2024). Second, there were errors related to the experiment due to detachment of the cells (Clavijo et al. 2007), a common problem observed in this cell line, which may have led to overestimation of viability.

The absence of cytotoxic effects and biocompatibility observed in these results was consistent with those of previous studies. Yu et al. (2020) found that metformin-loaded PLGA microspheres did not significantly affect the viability of 3T3-L1 cells except at undiluted concentrations. Wang et al. (2023) demonstrated that aptamer-functionalized PEG-PLGA NPs at doses of 5-30 µg/mL were biocompatible with these cells. These findings underscore the potential of PLGA NPs as safe vehicles for the delivery of active compounds, reaffirming their

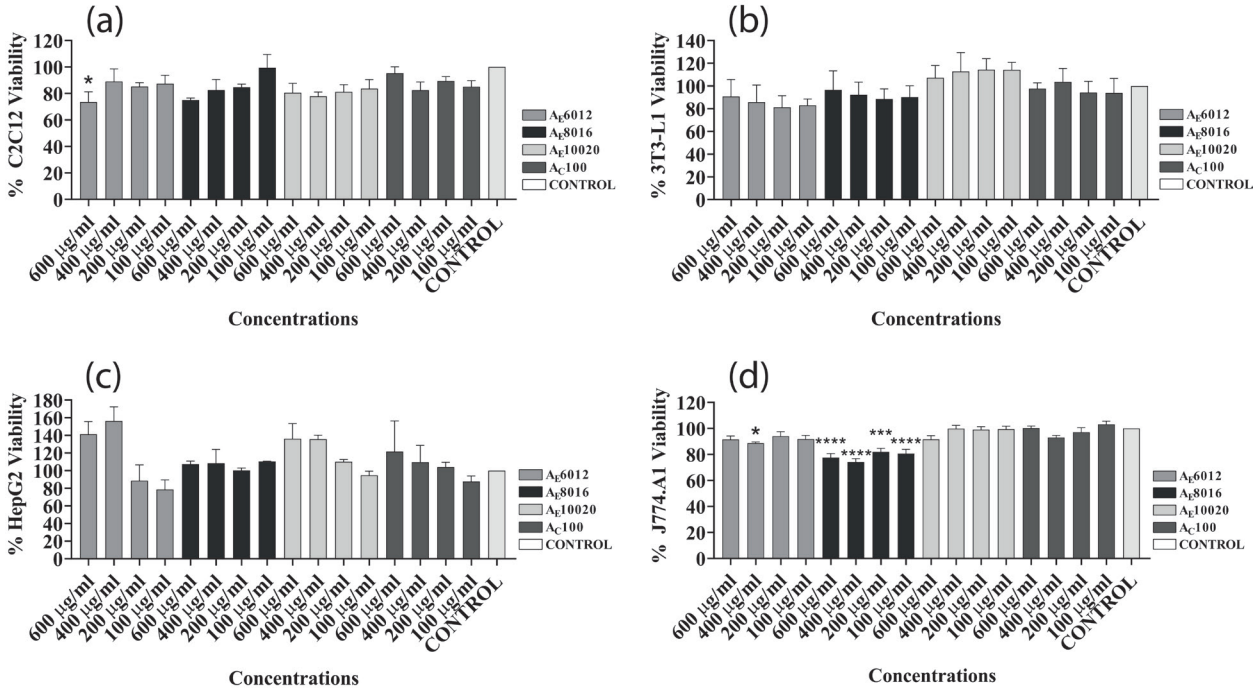

Figure 4. Viability of C2C12 (a), 3T3-L1 (b), HepG2 (c), and J774.A1 (d) cell lines were treated with PLGA NPs encapsulated in OBE100 (AE6012, AE801,6, and AE10020) and unencapsulated (AC100) at concentrations of 60 L, 40 L, 20, and 100 µg/mL. Statistical significance is indicated at P < 0.05, *** P < 0.0001, and **** P < 0.0001.

ability to maintain favourable interactions with cells without inducing cytotoxicity.

Cell viability in HepG2

The viability of HepG2 cell line treated with OBE100-encapsulated (A_E6012, A_E8016, and A_E10020) or non-encapsulated (A_C100) PLGA NPs are shown in Figure 4c. Comparison between NP-treated cells and the viability of untreated control cells showed no statistically significant differences (P > 0.05), with viabilities ranging from 78.5 ± 10.9% to 141 ± 14.3%, indicating that the NPs did not affect the viability of the cell line. In addition, viability percentages higher than 100% were observed for these NPs, possibly because of the proliferative effect of the PLGA polymer (Yu et al. 2020, Yan et al. 2024), which was similar to the effect observed in the 3T3-L1 line (adipocytes).

These results are in agreement with those conducted by Paul et al. (2013) and Silva et al. (2019), who showed that neither unencapsulated PLGA NPs nor PLGA NPs loaded with chelidonia and triterpenes exhibited significant cytotoxicity in hepatocytes, even at high concentrations.

Cell viability in J774A.1

The viability of the J774.A1 cell line treated with OBE100-encapsulated (A_E6012, A_E8016, and A_E10020) and non-encapsulated (A_C100) PLGA NPs in Figure 4d. Analyses indicated statistically significant differences (P < 0.05) when comparing viability with untreated control cells. These differences were associated exclusively with A_E8016 NPs, with viability percentages ranging from 74.2 ± 2.6% to 82.2 ± 2.6%, without affecting cell viability.

These results are consistent with those reported by Van de Ven et al. (2011), who evaluated PLGA NPs loaded with β-aescin and obtained close to 100% viability at a concentration of 129 µg/ml. Bitencourt et al. (2015) assessed

the viability of PLGA microspheres after 24 h of exposure, and found no cytotoxicity of J774.A1 line.

CONCLUSIONS

Optimization of the PLGA NPs preparation conditions allowed the preparation of OBE100-encapsulated PLGA NPs with particle sizes between 100 and 200 nm and low PDI. HPLC analysis showed that the highest EE was for AE6012 NPs, with 81.569 ± 1.798% and a particle size of 174.900 ± 1.539 nm, which are suitable for oral drug delivery. The ANOVA obtained in the multiple linear regression model using MSR was significant at $P < 0.05$. The R^2 values for these systems were higher than 0,85; this means that these models could explain the variability of more than 85% of each response variable.

The R^2 values for these systems were greater than 0.85, indicating that these models explained more than 85% of the variability in each response variable. The same was observed for the adjusted R^2, confirming that the linear regression model fit the experimental data used to construct the response surface and contour plots. The multiple linear regression equation obtained for the response variables (size, PDI, PZ, PZ, LC, and EE) showed a reduction or increase when the variables X(PLGA) and Y(OBE100) were used individually and in combination with X*Y (PLGA*OBE100). This confirmed the influence of each of the independent variables in the standardization and optimization process. The optimum point reached by the MSR for the response variables (size, PDI, and PZ) was at a ratio of PLGA 100 mg and OBE100 12 mg, obtaining sizes around 110.07 nm, PDI value of 0.14, and PZ value of -43.12 mV. For CC, the optimum point was 2.24% when the coefficient of the PLGA variable was 100 mg with an OBE100 of 20 mg. In contrast, the optimum point for the variable of interest EE was 80%, which was reached when the coefficient for the PLGA variable was 60 mg and that for OBE100 was 12 mg, confirming the fit of the results to these conditions. Therefore, the possibility of using PLGA: OBE100 ratios of 100:12 (mg), 100 mg: 20 mg, and 60 mg: 12 mg remains open for future large-scale standardization tests.

Cell viability assays were performed using C2C12, 3T3-L1, HepG2, and J774.A1 cell lines showed that NPs administered at concentrations of 600, 400, 200 and 100 µg/ml, maintained viability above 70%, indicating low cytotoxicity. These results suggest that the concentrations evaluated are not only safe but also suitable for future research on their biological activity.

These results suggest that PLGA NPs are promising therapeutic alternatives for the management of type 2 diabetes mellitus, obesity, and metabolic complications, taking advantage of the potential of natural products for the production of safe and effective drugs.

In the development of drugs and nutraceuticals, it is essential to navigate the various stages established by international organizations to ensure the creation of high-quality products. This study marks the beginning of the development process of a nanoformulation that aims to possess high therapeutic efficacy and low toxicity in addressing obesity and type 2 diabetes (DM2). After assessing the physicochemical properties of the formulation and evaluating them in cellular models relevant to these conditions, we will proceed with effectiveness and safety tests using a murine model of diet-induced obesity and insulin resistance.

Acknowledgments

We thank MINCIENCIAS for funding this research Project: Pre-clinical evaluation of a natural extract-based nanoformulation with potential antiobesogenic and antidiabetic activity (code 84357) of the call 896-2021 for

the strengthening of regional health research capacities in Colombia. The data supporting the findings of this study are available from the corresponding author (Norman Balcazar Morales) upon request.

REFERENCES

ACÍN S, MUÑOZ D, GUILLÉN A, SOSCUE D, CASTAÑO A, ECHEVERRI F & BALCAZAR N. 2021. Triterpene-enriched fractions from Eucalyptus tereticornis ameliorate metabolic alterations in a mouse model of diet-induced obesity. J Ethnopharmacol 265: 113298.

ADEBILEJE T, VALIZADEH A & AMANI A. 2017. Effect of formulation parameters on the size of PLGA nanoparticles encapsulating bovine serum albumin: a response surface methodology. J Contemp Med Sci 3(12): 306-312.

ALEGRÍA-EZQUERRA E, CASTELLANO-VÁZQUEZ JM & ALEGRÍA-BARRERO A. 2008. Obesidad, síndrome metabólico y diabetes: implicaciones cardiovasculares y actuación terapéutica. Rev Esp Cardiol 61(7): 752-764.

ALFEI S, SCHITO AM & ZUCCARI G. 2021. Considerable improvement of ursolic acid water solubility by its encapsulation in dendrimer nanoparticles: Design, synthesis and physicochemical characterization. Nanomaterials 11: 2196.

ALIREZAEI M, GHOBEH M & ES-HAGHI A. 2022. Poly(lactic-co-glycolic acid)(PLGA)-based nanoparticles modified with chitosan-folic acid to delivery of Artemisia vulgaris L. essential oil to HT-29 cancer cells. Process Biochem 121: 207-215.

ANWER MK, MOHAMMAD M, EZZELDIN E, FATIMA F, ALALAIWE A & IQBAL M. 2019. Preparation of sustained release apremilast-loaded PLGAlga nanoparticles: In vitro characterization and in vivo pharmacokinetic study in rats. Int J Nanomedicine 14: 1587-1595.

ARINMIŞ KN, KIYAN HT & ÖZTÜRK AA. 2024. Preparation, Characterization, Antioxidant Activities, and Determination of Anti-Alzheimer Effects of PLGA-Based DDSs Containing Ferulic Acid. ACS Omega 9(10): 11321-11338.

BITENCOURT CS, SILVA LB, PEREIRA PT, GELFUSO GM & FACCIOLI LH. 2015. Microspheres prepared with different co-polymers of poly(lactic-glycolic acid) (PLGA) or with chitosan cause distinct effects on macrophages. Colloids Surf B Biointerfaces 136: 678-686.

CLAVIJO M, GÓMEZ D & GÓMEZ C. 2007. Adipogenesis in vitro de celulas 3T3-L0000001. Rev Fac Med 15(2): 170-176.

CRUZ KP ET AL 2021. Development and Characterization of PLGA Nanoparticles Containing 17-DMAG, an Hsp90 Inhibitor. Front Chem 9: 644827.

ESCOBAR E, ACIN S, MUÑOZ DL, FERNÁNDEZ M, ECHEVERRI A, ECHEVERRI F, OROZCO J & BALCÁZAR N. 2023. Polymeric nanoformulation prototype based on a natural extract for the potential treatment of type 2 diabetes mellitus. J Drug Deliv Sci Technol 81: 104264.

GASPAR LM, DÓREA AC, DROPPA-ALMEIDA D, DE MÉLO-SILVA IS, MONTORO FE, ALVES LL, MACEDO MLH & PADILHA FF. 2018. Development and characterization of PLGA nanoparticles containing antibiotics. J Nanoparticle 20(11): 289.

GHARI T, MORTAZAVI SA, KHOSHAYAND MR, KOBARFARD F & GILANI K. 2014. Preparation, optimization, and in vitro evaluation of azithromycin encapsulated nanoparticles by using response surface methodology. J Drug Deliv Sci Technol 24(4): 352-360.

GOVARDHANE S & SHENDE P. 2024. Zinc-Phthalocyanine Loaded PLGA-PVA-Chitosan Nanosystem for the Enhancement of Antidiabetic Activity. J Mol Pharm 21(1): 62-75.

GUGLIELMI V, CARTON F, VATTEMI G, ARPICCO S, STELLA B, BERLIER G, MARENGO A, BOSHI F & MALATESTA M. 2019. Uptake and intracellular distribution of different types of nanoparticles in primary human myoblasts and myotubes. Int J Pharm 560: 347-356.

GUTIERREZ H & SALAZAR R. 2012. Análisis y diseño de experimentos. 3rd ed., McGrawHill.

HAIDER T & SONI V. 2022. Response surface methodology and artificial neural network-based modeling and optimization of phosphatidylserine targeted nanocarriers for effective treatment of cancer: In vitro and in silico studies. J Drug Deliv Sci Technol 75: 103663.

HEREDIA M & CABRIALES EC. 2022. Risk of type 2 diabetes mellitus and its determinants. Enferm Global 21(1): 179-190.

HO HN, TRAN TH, TRAN TB, YONG CS & NGUYEN CN 2015. Optimization and Characterization of Artesunate-Loaded Chitosan-Decorated Poly(D,L-lactide-co-glycolide) Acid Nanoparticles. Nanomaterials 2015: 1-12.

HU F, LIU W, YAN L, KONG F & WEI K. 2019. Optimization and characterization of poly(lactic-co-glycolic acid) nanoparticles loaded with astaxanthin and evaluation of anti-photodamage effect in vitro. R Soc Open Sci 6: 1911842.

IDF - INTERNATIONAL DIABETES FEDERATION. 2021. Diabetes Atlas. 10th ed., International Diabetes Federation.

ISO - INTERNATIONAL ORGANIZATION FOR STANDARDIZATION. 2009. Biological evaluation of medical devices. 3rd ed., International Organization for Standardization.

JASWIR I, NOVIENDRI D, TAHER M, MOHAMED F, OCTAVIANTI F, LESTARI W, MUKTI AG, NIRWANDAR S & HAMAD-ALMANSORI BB. 2019. Optimization and formulation of fucoxanthin-loaded microsphere (F-LM) using response surface methodology (RSM) and analysis of its fucoxanthin release profile. Molecules 24(5): 1-16.

JO A, RINGEL-SCAIA VM, MCDANIEL DK, THOMAS CA, ZHANG R, RIFFLE JS, ALLEN IC & DAVIS RM. 2020. Fabrication and characterization of PLGA nanoparticles encapsulating large CRISPR-Cas9 plasmid. J Nanobiotechnology 18: 1-14.

JUSU SM, OBAYEMI JD, SALIFU AA, NWAZOJIE CC, UZONWANNE V, ODUSANYA OS & SOBOYEJO WO. 2020. Drug-encapsulated blend of PLGA-PEG microspheres: in vitro and in vivo study of the effects of localized/targeted drug delivery on the treatment of triple-negative breast cancer. Sci Rep 10(1): 1-23.

KAMALY N, YAMEEN B, WU J & FAROKHZAD OC. 2016. Degradable controlled-release polymers and polymeric nanoparticles: Mechanisms of controlling drug release. J Am Chem Soc 116(4): 2602-2663.

LIU E, ZHAO S, LI X, MENG X & LIU B. 2021. Preparation, characterization of PLGA/chitosan nanoparticles as a delivery system for controlled release of DHA. J Biol Macromol 185: 782-791.

LU B, LV X & LE Y. 2019. Chitosan-modified PLGA nanoparticles for control-released drug delivery. Polymers 11(2): 304.

MALDONADO C, PANIAGUA N, BUSSMANN R, ZENTENO F & FUENTES A. 2020. The importance of medicinal plants, their taxonomy and the search for a cure for the disease caused by the coronavirus (COVID-19). Ecology of Bolivia 55(1): 2075-5023.

MEJÍA SP, SÁNCHEZ A, VÁSQUEZ V & OROZCO J. 2021. FunctionalNanocarriers for Delivering Itraconazole Against Fungal Intracellular Infections. Front Pharmacol 12: 685391.

MENDOZA N, ALCALÁ S & QUINTANAR D. 2016. Preparation of Polymer Nanoparticles by the Emulsification-Solvent Evaporation Method: From Vanderhoff's Pioneer Approach to Recent Adaptations. In Polymer Nanoparticles for Nanomedicines. Springer, 87-121 p.

PAUL A, DAS S, DAS J, SAMADDER A & KHUDA-BUKHSH AR. 2013. Cytotoxicity and apoptotic signalling cascade induced by chelidonine-loaded PLGA nanoparticles in HepG2 cells in vitro and bioavailability of nano-chelidonine in mice in vivo. Toxicol Lett 222(1): 10-22.

REDDIN IG, FENTON TR, WASS MN & MICHAELIS M. 2023. Large inherent variability in data derived from highly standardised cell culture experiments. Pharmacol Res 188: 1-3.

RUIZ E, OROZCO VH, HOYOS LM & GIRALDO LF. 2022. Study of sonication parameters on PLA nanoparticles preparation by simple emulsion-evaporation solvent technique. Eur Polym J 173: 1-11.

SAMANI S & TAGHIPOUR B. 2015. PLGA micro and nanoparticles in delivery of peptides and proteins; problems and approaches. Pharma Dev Tech 20(4): 385-393.

SANAPALLI BK, YELE V, SINGH MK, THUMBOORU SN, PARVATHANENI M & KARRI V. 2023. Human beta defensin-2 loaded PLGA nanoparticles impregnated in collagen-chitosan composite scaffold for the management of diabetic wounds. Biomed Pharmacother 161: 114540.

SÁNCHEZ A, MEJÍA SP & OROZCO J. 2020. Recent advances in polymeric nanoparticle-encapsulated drugs against intracellular infections. Molecules 25: 3760.

SILVA AM, ALVARADO HL, ABREGO G, MARTINS-GOMES C, GARDUÑO-RAMIREZ ML, GARCÍA ML, CALPENA AC & SOUTO EB. 2019. In Vitro Cytotoxicity of Oleanolic/Ursolic Acids-Loaded in PLGA Nanoparticles in Different Cell Lines. Pharmaceutics 11(8): 362.

SUN Y, CHEN D, PAN Y, QU W, HAO H, WANG X, LIU Z & XIE S. 2019. Nanoparticles for antiparasitic drug delivery. Drug Deliv 26(1): 1206-1221.

SURYA N & BHATTACHARYYA S. 2021. PLGA – the smart polymer for drug delivery. F Farmatsiya Farmako 9(5): 334-345.

VAN DE VEN H, VERMEERSCH M, MATHEEUSSEN A, VANDERVOORT J, WEYENBERG W, APERS S, COS P, MAES L & LUDWIG A. 2011. PLGA nanoparticles loaded with the antileishmanial saponin β-aescin: Factor influence study and in vitro efficacy evaluation. Int J Pharm 420(1): 122-132.

VICARI L, MUSUMECI T, GIANNONE I, ADAMO L, CONTICELLO C, DE MARIA R, PIGNATELLO R, PUGLISI G & GULISANO M. 2008. Paclitaxel loading in PLGA nanospheres affected the in vitro drug cell accumulation and antiproliferative activity. BMC Cancer 8: 1-11.

WAGHULDE M, MUJUMDAR A & NAIK J. 2019. Preparation and characterization of miglitol-loaded Poly (d, l-lactide-co-glycolide) microparticles using high pressure homogenization-solvent evaporation method. Int J Polym Mater Polym Biomater 68(4): 198-207.

WAN B, BAO Q & BURGESS D. 2023. Long-acting PLGA microspheres: Advances in excipient and product analysis toward improved product understanding. In Adv Drug Deliv Rev 198: 114857.

WANG Y, SONG W, LI Y, ZHOU Z, LI C, YU W & HE Y. 2023. Metformin-loaded PLGA microspheres combined with an in situ-formed injectable SA/BG hydrogel alleviate rotator cuff muscle degeneration. Mater Today Bio 23: 1-13.

WEISSIG V, PETTINGER TK & MURDOCK N. 2014. Nanopharmaceuticals (part 1): products on the market. Int J Nanomedicine 9: 4357-4373.

WISCHKE C & SCHWENDEMAN S. 2008. Principles of encapsulating hydrophobic drugs in PLA/PLGA microparticles. Int J Pharm 364(2): 298-327.

WHO - WORLD HEALTH ORGANIZATION. 2021. Obesity and overweight.

YAN B, HUA Y, WANG J, SHAO T, WANG S, GAO X & GAO J. 2024. Surface Modification Progress for PLGA-Based Cell Scaffolds. Polymers 16: 165.

YU B ET AL. 2020. Targeted delivery of emodin to adipocytes by aptamer-functionalized PEG-PLGA nanoparticles in vitro. J Drug Deliv Sci Technol 57: 101739.

YURTDAŞ-KIRIMLIOĞLU G. 2022. A promising approach to design thermosensitive in situ gel based on solid dispersions of desloratadine with Kolliphor® 188 and Pluronic® F127. J Therm Anal Calorim 147(2): 1307-1327.

How to cite

CELY-GARCIA MC, ESPINEL-PABÓN DY, JAIMES-MENDEZ N, BALCAZAR-MORALES N & MURILLO-RUIZ DA. 2025. Encapsulation of *Eucalyptus tereticornis* extract in polylactic-co-glycolic acid nanoparticles: standardization, optimization and cell viability. An Acad Bras Cienc 97: e20241069. DOI 10.1590/0001-3765202520241069.

Manuscript received on September 20, 2024; accepted for publication on January 17, 2025

MARIA C. CELY-GARCIA[1]
https://orcid.org/0009-0001-8047-7284

DIANA Y. ESPINEL-PABÓN[2]
https://orcid.org/0000-0002-7381-0085

NANCY JAIMES-MENDEZ[3]
https://orcid.org/0000-0001-8089-5358

NORMAN BALCAZAR-MORALES[4]
https://orcid.org/0000-0002-1860-1176

EDWIN A. MURILLO-RUIZ[5]
https://orcid.org/0000-0002-0617-2327

[1]Universidad Francisco de Paula Santander, Facultad de Ciencias Básicas, Grupo de Investigación en Materiales Poliméricos (GIMAPOL), Av. Gran Colombia, 12E-96, Cúcuta, Colombia

[2]Universidad de Pamplona, Facultad de Ciencias Básicas, Grupo de Investigación en Biología Molecular y Genética (BIOMOGEN), Campus Universitario, Km 1, Vía Bucaramanga, 543050, Pamplona, Colombia

[3]Universidad de Pamplona, Departamento de Biología, Grupo de Investigación en Biología Molecular y Genética (BIOMOGEN), Campus Universitario, Km 1, Vía Bucaramanga, 543050, Pamplona, Colombia

[4]Universidad de Antioquia, Departamento de Fisiología y Bioquímica, Facultad de Medicina, Grupo de Investigación de Genética Molecular (GENMOL), Calle 62 n° 52-59, Medellín, Colombia

[5]Universidad Francisco de Paula Santander, Departamento de Química, Grupo de Investigación en Materiales Poliméricos (GIMAPOL), Av. Gran Colombia, 12E-96, Cúcuta, Colombia

Correspondence to: **Norman Balcazar-Morales**
E-mail: norman.balcazar@udea.edu.co

Author contributions

The author (s) have (has) accepted responsibility for the entire content of this manuscript and approved its submission. MCCG contributed to the encapsulation process, physicochemical characterization, standardization, optimization of the encapsulation process, evaluation and discussion of the results, and the writing of the original manuscript. NBM contributed to the study of cell viability and the evaluation and discussion of the results. DYEP contributed to the study of cell viability, evaluation, and discussion of the results, and writing of the original manuscript. NJM contributed to the study of cell viability and discussion of the results. EAMR contributed to the encapsulation process, physicochemical characterization, evaluation, discussion of the results, and writing of the original manuscript. All authors provided conceptualization, methodology, and critical feedback, and helped shape the manuscript and literature review.